

CHANGES IN SOLID-STATE CELLULOSE NANOFIBERS INDUCED BY GAMMA-RAY IRRADIATION: COMPARATIVE EVALUATION OF PURE AND LIGNIN/HEMICELLULOSE-CONTAINING STRUCTURES

TARO KINUMOTO,^{*,**} YUKINO MASUDA,^{***} KEISUKE TOJO,^{***} MIKI MATSUOKA^{*} and MASAYA MORIYAMA^{*}

^{*}*Applied Chemistry Cluster, Faculty of Science and Technology, Oita University
700 Dannoharu, Oita, 870 1192, Japan*

^{**}*Research Center for Advanced Technology and GX, Oita University,
700 Dannoharu, Oita, 870-1192, Japan*

^{***}*Applied Chemistry Course, Graduate School of Engineering, Oita University,
700 Dannoharu, Oita, 870-1192, Japan*

✉ Corresponding author: T. Kinumoto, kinumoto@oita-u.ac.jp

Received August 25, 2025

In this study, the effects of gamma-ray irradiation on the physicochemical properties of cellulose nanofiber (CNF) and lignin/hemicellulose-containing cellulose nanofiber (LHCNF) were investigated. Solid-state CNF (SS-CNF) and solid-state LHCNF (SS-LHCNF) sheets were prepared and irradiated with gamma-rays at doses of 60 and 300 kGy. Fourier transform infrared (FT-IR) and X-ray diffraction (XRD) analyses revealed no significant changes in the chemical structure or crystallinity. These results suggest that the chemical changes (damage) are minor and cannot be confirmed by the available instruments. Tensile testing showed a dose-dependent decrease in the maximum stress for both types of CNF sheets, indicating radiation-induced damage. However, while the elastic modulus of SS-CNF decreased with increasing irradiation dose, SS-LHCNF retained approximately 90% of its modulus, even after 300 kGy, demonstrating higher mechanical stability. Thermogravimetric analysis further revealed that the 1% weight-loss temperature decreased monotonically with irradiation dose for SS-CNF, whereas SS-LHCNF showed only a moderate decrease between 60 and 300 kGy. These results highlight that the presence of lignin and hemicelluloses (and their derivatives) in LHCNF influences the extent of changes in physicochemical properties induced by gamma-ray irradiation.

Keywords: gamma-ray irradiation, cellulose nanofibers, lignin, hemicelluloses

INTRODUCTION

Biorefinery technologies based on plant-derived resources are expected to provide sustainable alternatives to petroleum-based industries, thereby contributing to the realization of a sustainable society and achievement of the Sustainable Development Goals (SDGs). Various plant resources, including softwood, hardwood, annual plants, and agricultural residues, have attracted considerable attention owing to their ability to fix carbon dioxide and their biodegradability. These resources are also promising raw materials for nanomaterials, such as cellulose nanofibers (CNFs) and cellulose nanocrystals (CNCs), which have recently garnered significant interest.¹⁻⁴

Research on CNFs and CNCs has expanded

rapidly in recent years, particularly with respect to production processes, physicochemical properties, and potential applications.¹⁻⁴ A wide range of CNF and CNC types have been developed, with their properties strongly influenced by the raw material and preparation method employed.¹⁻⁴ Among them, 2,2,6,6-tetramethylpiperidine-1-oxyl (TEMPO)-oxidized CNF (TOCNF), typically 3–4 nm in diameter, is frequently employed in CNF-related studies.¹⁻⁴ However, TOCNF is classified as an oxidized cellulose because the hydroxy group at the C6 position of the glucose unit is converted to a carboxy group.

We previously reported the preparation of cellulose-based CNF (>95% cellulose) from

bamboo (CELEENA™).⁵ Its thermal decomposition point (TDP) exceeds 260 °C, which is considerably higher than that of TOCNF (approximately 222 °C) and comparable to that of native cellulose (approximately 275 °C).⁶ This difference arises from the introduction of carboxy groups at the C6 position in TOCNF.⁴ Thus, CELEENA is considered an ideal material for investigating the intrinsic physical properties of nanocellulose, as it preserves the native characteristics of cellulose, in contrast to chemically modified products, such as TOCNF. CELEENA is commercially available from Oita CELEENA Co. Ltd., Japan.⁷

In our previous work, we prepared solid-state CNF (SS-CNF) sheets from highly pure CNF and investigated their response to gamma-ray irradiation up to 300 kGy.⁵ No significant changes in chemical structure were observed before and after the irradiation; however, the thermal stability slightly decreased at 60 kGy, and both the mechanical strength and thermal stability deteriorated substantially after 300 kGy.

In addition to cellulose, plants such as trees and bamboo contain large amounts of lignin and hemicelluloses. While CNFs are typically produced by isolating cellulose from plant biomass, lignin- and hemicellulose-containing CNF (LHCNF) can also be prepared by retaining these components.⁸ Motivated by this, we investigated the effects of gamma-ray irradiation on CNFs containing lignin and hemicelluloses. Specifically, LHCNF was prepared from bamboo powder as a raw material, fabricated into solid-state LHCNF (SS-LHCNF) sheets, and subjected to gamma-ray irradiation under the same conditions as those used in our previous study.⁵ This work compares the changes in properties between CNF and LHCNF upon irradiation and

discusses the influence of lignin and hemicelluloses on their physicochemical behavior.

It should be noted that we previously reported the maximum stress and elastic modulus of lignin- and hemicellulose-containing CNFs.⁹ However, the present results differ owing to the use of different raw material forms.^{5,9} Specifically, we used bamboo fibers as the raw material of CNF and LHCNF in our previous studies,^{5,9} while we have newly developed CNF and LHCNF using bamboo powder as a raw material in this study. Therefore, the results differed because the fiber lengths of the raw materials differed. Moreover, one of our previous studies did not include chemical information such as Fourier transform infrared (FT-IR), X-ray diffraction (XRD), number-average degree of polymerization, or thermal properties.⁹ Therefore, this study presents new data and provides a detailed chemical analysis of the effects of gamma-ray irradiation on both CNF and LHCNF.

EXPERIMENTAL

CNF and LHCNF

CNF and LHCNF were prepared with the support of Oita CELEENA Co., Ltd. Aqueous suspensions containing approximately 1 wt% CNF or LHCNF were obtained using a bamboo-based production process. The CNF suspension appeared shiny white, whereas the LHCNF suspension was brownish, which was attributed to the lignin-derived components. The difference in color can be confirmed by the difference in the color tones shown in Figures 1 (a) and 2 (a). The compositions of both CNF samples were determined by the detergent analysis method at Tokai Techno Co., Ltd. (Table 1).¹⁰

The details of the detergent method for determination of the composition ratios of cellulose, hemicelluloses, and lignin are provided below.

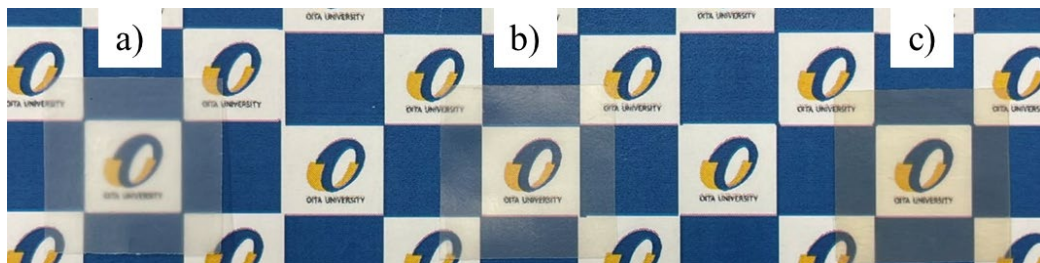


Figure 1: Appearances of SS-CNF before irradiation (a), and after irradiation at 60 (b) and 300 kGy (c)

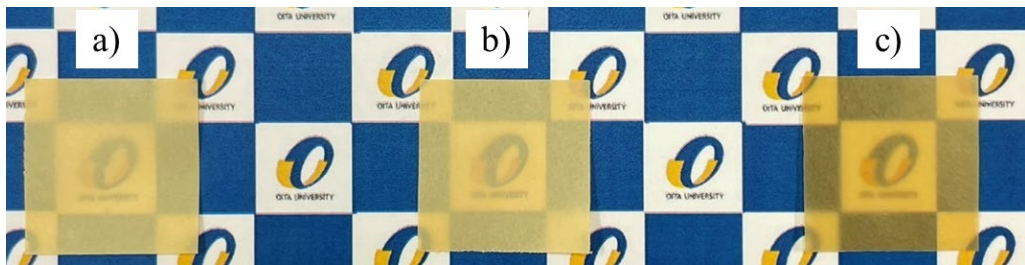


Figure 2: Appearances of SS-LHCNF before irradiation (a), and after irradiation at 60 (b) and 300 kGy (c)

Table 1
Composition of CNF and LHCNF

Sample	Composition (%)		
	Cellulose	Hemicelluloses	Lignin
CNF	98	2	0
LHCNF	75	14	11

Moisture content

Approximately 2 g of the sample was taken and dried for a set time or until a constant weight was achieved. The moisture content (%-wet) was determined from the weight difference before and after drying.

Ash content

Approximately 2 g of the sample was taken and heated at 600 °C for 2 h. The ash content (%-dry) was determined from the weight difference before and after heating.

Neutral detergent fiber (NDF)

20 mL of pure water and approximately 0.5 g of sample were mixed and boiled for 30 min. After that, 20 mL of α -amylase solution (α -amylase dissolved in pH 5.8 phosphate buffer) was added, and starch hydrolysis was carried out at 40 °C for 16 h.

The residue was collected by filtration, 100 mL of a neutral detergent solution (consisting of disodium dihydrogen ethylenediaminetetraacetate dihydrate, sodium tetraborate decahydrate, disodium hydrogen phosphate, sodium n-dodecyl sulfate, and triethylene glycol dissolved in pure water) was added, and the mixture was boiled for 1 h, followed by filtration, washing, drying, and weighing. It was also further heated under the same conditions as in the ash content measurement and weighed. The NDF (%-dry) was determined by subtracting the ash from the dried residue.

Acid detergent fiber (ADF)

100 mL of Acid Detergent solution (cetyltrimethylammonium bromide dissolved in 1 L of ca. 4.5 wt% sulfuric acid) was added to the NDF dried residue, and the mixture was boiled for 1 h, followed by filtration, washing, drying, and weighing. It was also further heated under the same conditions as in the ash content measurement and weighed. The ADF (%-dry)

was determined by subtracting the ash from the dried residue.

Acid detergent lignin (ADL)

15 mL of 72% sulfuric acid was added to the ADF dried residue, and it was left to stand for 3 h (with occasional stirring). It was filtered and washed using pure water and boiling water, then dried and weighed. It was also further heated under the same conditions as in the ash content measurement and weighed. The ADL (%-dry) was determined by subtracting the ash from the dried residue.

Cellulose content

Cellulose (%-dry) was determined by the following formula:

$$\text{Cellulose (%-dry)} = \text{ADF (%-Dry)} - \text{ADL (%-Dry)} \quad (1)$$

Hemicellulose content

Hemicelluloses (%-dry) were determined by the following formula (2):

$$\text{Hemicelluloses (%-dry)} = \text{NDF (%-dry)} - \text{ADF (%-dry)} \quad (2)$$

Lignin content

Lignin (%-dry) was determined by the following formula:

$$\text{Lignin (%-dry)} = \text{ADL (%-dry)} \quad (3)$$

In this study, lignin and hemicelluloses are collectively referred to as lignin and hemicelluloses, although their derivatives are also present in LHCNF. The average diameters and standard deviations, estimated by field-emission scanning electron microscopy (FE-SEM), were approximately 18 ± 4.8 nm for CNF and 18 ± 6.7 nm for LHCNF, respectively.

Preparation of SS-CNF

SS-CNF and SS-LHCNF sheets were prepared without binders, following a previously reported method.⁵ Briefly, a predetermined volume of CNF or

LHCNF suspension was filtered using a vacuum filtration apparatus (UHP-76K, Advantec Toyo) with a membrane filter (pore size = 1.0 μm , diameter = 90 mm, H100A090C, Advantec Toyo). The resulting wet cake was carefully removed, lightly dried, and subsequently hot-pressed at 110 °C using a hot press machine (AH-2003, AS ONE Corporation) to obtain circular sheets with a normalized thickness of approximately 50 μm . Representative images of the SS-CNF and SS-LHCNF sheets are shown in Figures 1 (a) and 2 (a).

Gamma irradiation and characterization of SS-CNF

Gamma irradiation of both SS-CNF and SS-LHCNF sheets was carried out under ambient conditions at the Chiyoda Technol ^{60}Co irradiation facility, Laboratory for Zero-Carbon Energy, Institute of Innovative Research, Tokyo Institute of Technology (now called Institute of Science Tokyo). Consistent with previous work, total doses of 60 and 300 kGy were applied.⁵ The irradiation conditions were determined based on a study by Sugimatsu *et al.* that used unbleached kraft pulp.¹¹ Our earlier study demonstrated that SS-CNF sheets exhibited slight changes in physicochemical properties after 60 kGy irradiation, whereas significant deterioration was observed at 300 kGy.⁶ In this study, we aimed to clarify the differences in irradiation responses between SS-LHCNF and SS-CNF.

Changes in the chemical structure before and after irradiation were examined by FT-IR spectroscopy (Nicolet iS5 FT-IR, Thermo Scientific) using the attenuated total reflection (ATR) method with a diamond prism and by XRD (MiniFlex-600, Rigaku) with CuK α radiation. The FT-IR spectra were recorded in the region of 4000–550 cm^{-1} at 4 cm^{-1} resolution with 32 scans. The XRD patterns were obtained in the 20 range from 10° to 80° with a step of 0.02°.

Tensile testing was performed using a mechanical testing system comprising a digital force gauge (ZTA-50N) and test stand (MX2-500N, Imada). Rectangular specimens (40 mm × 10 mm, thickness ~50 μm , weight ~20 mg) were cut from the SS-CNF and SS-LHCNF

sheets. Tests were conducted at room temperature (24–26 °C) under ambient humidity (43–47% RH). Each specimen was mounted with 10 mm on each side clamped, leaving a 20 mm gauge length, and extended at a crosshead speed of 10 mm min^{-1} . The tensile strength and elastic modulus were calculated from the load–displacement data, and average values with standard deviations were obtained from multiple measurements.

RESULTS AND DISCUSSION

Appearance

Figures 1 (b, c) and 2 (b, c) show the appearance of SS-CNF and SS-LHCNF sheets after irradiation at 60 and 300 kGy, respectively. The SS-CNF sheets gradually turned yellow with an increasing irradiation dose. By contrast, the color change of the SS-LHCNF sheets was not readily apparent, probably because their initial brown coloration masked any additional changes. Therefore, the yellowing of the SS-CNF was attributed to minor radiation-induced damage to cellulose.⁵

FT-IR spectra

Figure 3 shows the FT-IR spectra of the SS-CNF and SS-LHCNF sheets before and after irradiation. The spectrum of the virgin SS-CNF sheet (Fig. 3 (a)) exhibited only typical cellulose absorption peaks, such as those at 3300, 2900, and 1100 cm^{-1} , corresponding to O–H, C–H, and C–C–O stretching vibrations, respectively. The spectra obtained after irradiation at 60 and 300 kGy (Fig. 3 (b, c)) showed no significant changes compared with the virgin sample, although the sheet color became slightly yellow. In addition, the notable structural indices such as crystallinity estimated from FT-IR spectra did not change after gamma-ray irradiation.^{12,13}

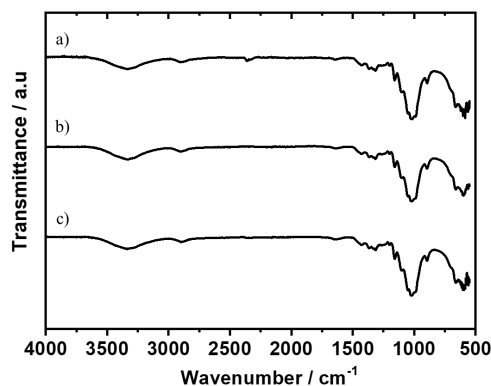


Figure 3: FT-IR spectra of SS-CNF before irradiation (a), and after irradiation at 60 (b) and 300 kGy (c)

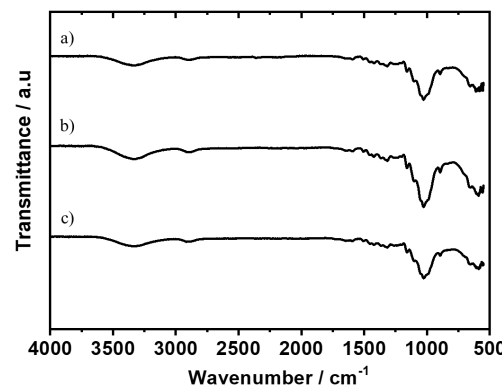


Figure 4: FT-IR spectra of SS-LHCNF before irradiation (a), and after irradiation at 60 (b) and 300 kGy (c)

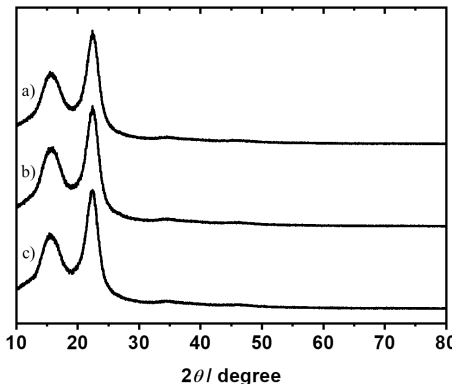


Figure 5: XRD patterns of SS-CNF sheet before irradiation (a), and after irradiation at 60 (b) and 300 kGy (c)

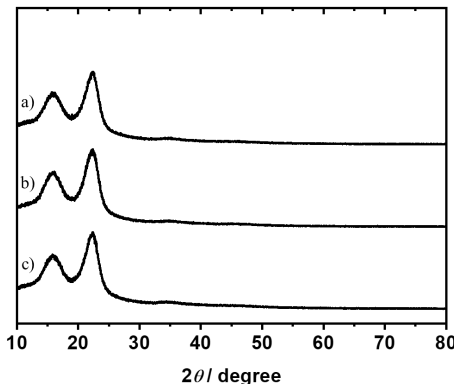


Figure 6: XRD patterns of SS-LHCNF sheet before irradiation (a), and after irradiation at 60 (b) and 300 kGy (c)

Table 2
Crystallinity indices of SS-CNF and SS-LHCNF

Sample	Crystallinity index (%)		
	Before	60 kGy	300 kGy
SS-CNF	80.2	80.7	80.2
SS-LHCNF	78.9	80.7	78.1

These results suggest that the chemical changes (damage) are minor and cannot be confirmed by the available FT-IR instrument.

The spectrum of the virgin SS-LHCNF sheet (Fig. 4 (a)) differed from that of SS-CNF, displaying characteristic lignin-derived peaks, particularly a strong absorption band near 1500 cm^{-1} assigned to aromatic skeletal vibrations. Because lignin is the only constituent that contains aromatic ring structures, this band is diagnostic. Notably, these lignin-associated peaks remained visible even after 300 kGy irradiation (Fig. 4 (b, c)), indicating the structural resilience of the lignin moieties under the applied conditions. Although LHCNF also contains hemicelluloses, its polysaccharide structure is similar to that of cellulose, and most of its absorption bands overlap with those of cellulose, making hemicellulose-specific peaks difficult to resolve.

XRD patterns

The XRD patterns of SS-CNF and SS-LHCNF before and after irradiation are shown in Figures 5 and 6, respectively. Both exhibited the cellulose I polymorph, and no distinct differences were observed between the samples or irradiation doses. The crystallinity indices were calculated according to the method of Isogai and Ueda,¹⁴ and the results are summarized in Table 2. The crystallinity indices of SS-CNF and SS-LHCNF were

comparable, suggesting that the crystalline regions of cellulose were not significantly affected by gamma irradiation.

Maximum stress and elastic modulus

Figure 7 shows the maximum stress and elastic modulus of the SS-CNF (■) and SS-LHCNF (●) sheets with respect to the total dose of gamma irradiation, plotted as average values from multiple measurements. Prior to irradiation, the maximum stress and elastic modulus of SS-CNF were higher than those of SS-LHCNF. For both materials, the maximum stress decreased progressively with increasing irradiation dose, by approximately 20% at 60 kGy and approximately 40% at 300 kGy, regardless of the lignin and hemicellulose content.

To clarify this, the molecular weight of cellulose in the SS-CNF was measured using gel permeation chromatography (GPC) at the Tosoh Analysis and Research Center Co., Ltd. A calibration curve was established using pullulan (Shodex) standards and the results were reported as pullulan equivalent values. The estimated molecular weights are presented in Table 3.

Discussion

Before gamma irradiation, the average molecular weight (M_n) of cellulose in the SS-CNF was 1.20×10^4 . After irradiation at 300 kGy, M_n decreased to 0.51×10^4 , corresponding to a

reduction of approximately 50%. In our previous study, CNF dispersions in water were irradiated with 60 kGy of gamma-rays and subsequently observed by FE-SEM, which revealed fiber fracture.⁵ The experimental conditions of the present work differed from those of the previous study in that irradiation was performed in ambient air rather than in aqueous suspension. Although

experiments at 300 kGy in aqueous conditions were not conducted, it is reasonable to assume that the extent of damage in water would be more severe than that observed at 60 kGy owing to the generation of reactive species from water radiolysis that can attack and cleave cellulose chains.

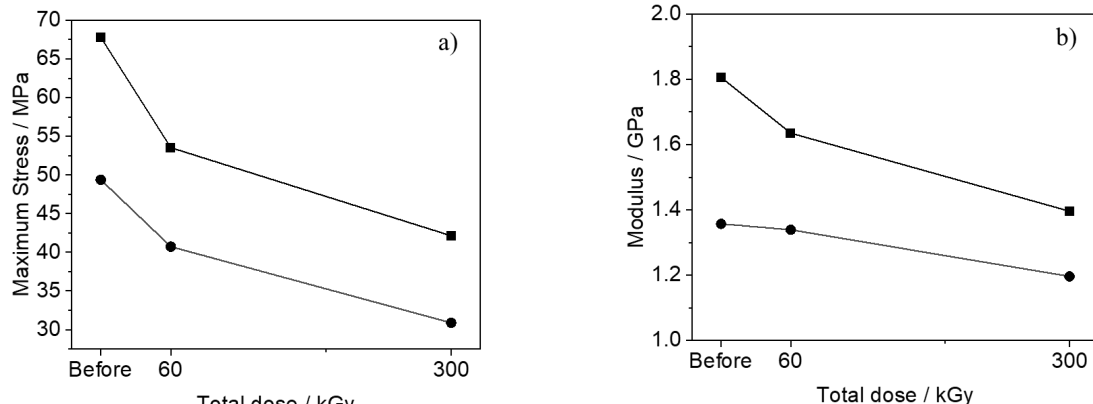


Figure 7: a) Maximum stress and b) elastic modulus of (■) SS-CNF and (●) SS-LHCNF sheets upon total dose of gamma irradiation

Table 3
Estimated molecular weight (M_n) of SS-CNF before and after irradiation at 300 kGy

CNF	$M_n (x10^4)$	
	Before	300 kGy
	1.20	0.51

Liu *et al.* demonstrated that gamma irradiation of microcrystalline cellulose facilitates its decomposition and results in a reduced degree of polymerization.¹⁵ They attributed this reduction primarily to oxidative decomposition and chain scission processes. The observed decrease in the degree of polymerization in the present study is considered to have occurred through a mechanism consistent with their findings.

This reduction in molecular weight is hypothesized to contribute to the observed decrease in the maximum stress. Upon gamma irradiation, the cellulose molecular chains in the SS-CNF undergo scission. Although the overall crystallinity did not appear to change in the average macroscopic structure detected by XRD, microscopic-level damage was likely to occur. Such molecular degradation is considered responsible for the reduction in the maximum stress, and additional microscopic defects may also have occurred. A similar trend in stress reduction was observed for SS-LHCNF. Although SS-LHCNF contains lignin and hemicelluloses, its

primary structural backbone is cellulose, and the damage induced by gamma irradiation is comparable to that of SS-CNF.

However, the change in elastic modulus differed between SS-CNF and SS-LHCNF. In SS-CNF, the elastic modulus decreased with increasing irradiation dose, similar to the trend observed for the maximum stress. After 300 kGy irradiation, the elastic modulus was reduced to approximately 80% of its pre-irradiation value. This reduction is primarily attributed to the cleavage of the cellulose molecular chains, as noted above, and the resulting molecular-level structural changes. Whereas the elastic modulus of SS-LHCNF was largely maintained up to 60 kGy; and even at 300 kGy, it decreased by approximately 10%, corresponding to a retention of approximately 90%.

LHCNF contains lignin and hemicelluloses (and their derivatives), which are believed to interact closely with cellulose molecules, as suggested by the microstructure of bamboo. In a simplified model, if bonds exist between cellulose and hemicelluloses, as well as between

hemicelluloses and lignin, the extent of hydrogen bonding among the cellulose microfibrils would be reduced. This structural characteristic is probably one of the main reasons why the maximum stress and elastic modulus prior to irradiation were higher for CNF than for LHCNF. Park *et al.* also found that cellulose nanofibers (such as CNF in this study) have greater maximum stress and elastic modulus than lignocellulose nanofibers (such as LHCNF in this study), attributing this to lignin's interference with hydrogen bonding between cellulose molecules.¹⁶

It is technically difficult to determine the molecular weight of each individual component of LHCNF. Nevertheless, as discussed above, cellulose, the primary structural backbone of LHCNF, may sustain gamma-ray-induced damage to an extent comparable to that of SS-CNF. However, the reduction in the elastic modulus was less pronounced than that of the maximum stress, suggesting the presence of an additional mechanism that mitigates the decrease in modulus.

Lignin differs from cellulose and hemicelluloses because it is composed of randomly polymerized monomeric lignols, which are phenolic derivatives. Its structure varies depending on the plant species and growth conditions and thus cannot be uniquely defined. The representative structural units of lignin are p-hydroxyphenyl (H), guaiacyl (G), and syringyl (S) nuclei.¹³ These structural features differ from those of cellulose and hemicelluloses, and their physicochemical properties vary accordingly. The FT-IR equipment used in this study was not sufficiently sensitive to

detect changes in lignin components induced by gamma-ray irradiation. Although a direct investigation of structural changes is currently not feasible, we decided to investigate the structural changes based on the results of thermogravimetry relating to the different thermal properties of lignin and cellulose.

Figure 8 shows the 1% weight-loss temperature before irradiation, after 60 kGy irradiation, and after 300 kGy irradiation. The 1% weight-loss temperature was defined as the temperature at which SS-CNF and SS-LHCNF lost 1% of their weight. Prior to irradiation, the 1% weight-loss temperature of LHCNF, which contains lignin and hemicelluloses, was lower than that of SS-CNF because lignin has the lowest thermal decomposition onset temperature among the three components.¹³

The thermal stability of SS-CNF decreased monotonically with increasing irradiation dose, likely owing to the cleavage and degradation of the cellulose molecular chains. By contrast, the 1% weight-loss temperature of SS-LHCNF decreased more gradually from 60 to 300 kGy. Although no direct correlation was evident, this trend resembled a change in the elastic modulus. If lignin was simply decomposed by gamma-ray irradiation, the 1% weight-loss temperature would be expected to continue decreasing. The gradual changes in elastic modulus and thermal stability indicate another chemical mechanism at work, beyond simple lignin decomposition reported by Brebu and Vasile.¹⁷

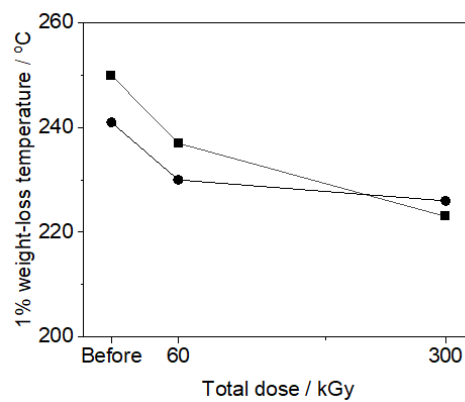


Figure 8: 1% weight-loss temperature of (■) SS-CNF and (●) SS-LHCNF sheets upon total dose of gamma irradiation

For SS-CNF, the thermal stability monotonically decreased as the total irradiation dose increased. This is likely due to the breakage and degradation of the cellulose molecular chains. By contrast, the 1% weight loss temperature of SS-

LHCNF gradually decreased from 60 to 300 kGy. Although it is unclear whether a direct correlation exists, it is very similar to the change in the elastic modulus. If lignin was simply decomposed by gamma-ray irradiation, the 1% weight loss

temperature would continue to decrease. However, gradual changes in the elastic modulus and thermal stability suggest an additional chemical mechanism other than decomposition.

Lignin is composed of randomly polymerized monolignols with various functional groups, such as hydroxy (OH), alkoxy (OR), and carboxy (COOH) groups, present in its side chains. Rao *et al.* reported that gamma-ray irradiation of kraft lignin induces dissociation and decomposition of OH groups from phenolic, alcoholic, glycosidic, and acetal oxygen moieties, leading to cleavage of C–O–C bonds and the generation of primary radicals, ultimately resulting in a reduction of molecular weight.¹⁸ Although the structures of lignin and kraft lignin contained in bamboo-derived LHCNF may differ, their report suggests that gamma irradiation generates primary radicals. Additionally, it has also been reported that irradiation cross-links cellulose and lignin, and changes in the bonding state of these three components may also influence the decrease in elastic modulus.¹⁹ However, as shown in Figure 7 (b), these effects appear to be less pronounced than the changes observed in the elastic modulus and stiffness of SS-CNF. This suggests that the interaction of lignin and hemicelluloses between the cellulose molecules may mitigate the reduction in elastic modulus.

Consequently, the influence of hemicelluloses on LHCNF, along with that of lignin, requires consideration. A more comprehensive understanding of the reduction in elastic modulus can be achieved by isolating hemicelluloses and lignin and clarifying their respective responses to gamma-ray irradiation. However, isolating these components from the LHCNF, while preserving their structural integrity, remains challenging. As a next step, we aim to investigate CNF composed of hemicelluloses and cellulose, and the results will be reported in a future work.

CONCLUSION

This study comprehensively evaluated the effects of gamma irradiation on highly pure CNF and lignin/hemicellulose-containing CNF (LHCNF) sheets.

Both SS-CNF and SS-LHCNF exhibited a decrease in the maximum stress with increasing irradiation dose. This might be primarily attributed to the scission of cellulose molecular chains, indicating that the main cellulose backbone in LHCNF sustained damage comparable to that in SS-CNF, despite the presence of lignin and

hemicelluloses.

The elastic modulus of SS-CNF decreased with increasing irradiation dose, whereas SS-LHCNF exhibited a higher retention rate than SS-CNF. This suggests that lignin and hemicelluloses contribute to mitigating the reduction in elastic modulus.

The thermal stability of SS-CNF decreased monotonically with the irradiation dose, whereas that of SS-LHCNF showed a moderate decrease from 60 to 300 kGy. This behavior implied the involvement of additional chemical mechanisms beyond simple degradation, such as condensation or cross-linking reactions associated with lignin molecules under gamma irradiation.

Overall, these results highlight the important roles of lignin and hemicelluloses in the gamma radiation resistance of CNF materials. In particular, the mechanism by which lignin and hemicelluloses suppress the reduction in the elastic modulus may provide new opportunities for the development of radiation-resistant nanocellulose composite materials. Future studies should aim to gain a more detailed understanding of the mechanism of elastic modulus reduction suppression by preparing and investigating the gamma irradiation properties of CNF composed solely of hemicelluloses and cellulose.

ACKNOWLEDGEMENT: The authors thank Dr. Isao Yoda of Tokyo Institute of Technology for assistance with gamma-ray irradiation and Oita CELEENA Co., Ltd. for their assistance with the preparation of CNF and LHCNF. This research was partially supported by the START Program (program for creating start-ups from advanced research and technology) of the Japan Science and Technology Agency under award number JPMJST1813, the JST Adaptable and Seamless Technology Transfer Program through Target-driven R&D (A-STEP) Grant Number JPMJTM20SQ, and the Oita University President's Strategic Discretionary Fund.

REFERENCES

- ¹ <https://www.sciencedirect.com/topics/materials-science/nanocellulose>
- ² A. Isogai, *J. Fiber Sci. Technol.*, **76**, 310 (2020), <https://doi.org/10.2115/fiberst.2020-0039>
- ³ T. Yi, H. Zhao, Q. Mo, D. Pan, Y. Liu *et al.*, *Materials*, **13**, 5062 (2020), <https://doi.org/10.3390/ma13225062>
- ⁴ N. V. Ehman, Q. Tarres, M. Delgado-Aguilar, M. Vallejos, F. Felissia, *et al.*, *Cellulose Chem. Technol.*, **50**, 361 (2016), <https://www.cellulosechemtechnol.ro/pdf/CCT3->

4(2016)/p.361-367.pdf

⁵ T. Kinumoto, M. Noda, M. Matsuoka, K. Kai, R. Takayama *et al.*, *Cellulose Chem. Technol.*, **56**, 543 (2022),

<https://doi.org/10.35812/CelluloseChemTechnol.2022.56.46>

⁶ H. Fukuzumi, T. Saito, Y. Okita and A. Isogai, *Polym. Degrad. Stabil.*, **95**, 1502 (2010),

<https://doi.org/10.1016/j.polymdegradstab.2010.06.01>.

⁷ <https://www.oitaceleena.co.jp/>

⁸ Y. Kojima, A. Isa, H. Kobori, S. Suzuki, H. Ito *et al.*, *Materials*, **7**, 6853 (2014),

<https://doi.org/10.3390/ma7096853>

⁹ T. Kinumoto, M. Noda, Y. Masuda, K. Kai, M. Moriyama *et al.*, *Nihon Koukuu Uchiyuu Gakkaishi*, **72**, 214 (2024), https://doi.org/10.14822/kjsass.72.6_214

¹⁰ <https://www.tokai-techno.co.jp/product-service/survey-and-analysis/er-analysis/cellulose/>

¹¹ A. Sugimatsu, S. Senda and Y. Harada, *Kogyokagakuzasshi*, **62**, 90 (1959)

¹² I. Reiniati, A. N. Hrymak and A. Margaritis, *Biochem. Eng. J.*, **127**, 21 (2017),

<https://doi.org/10.1016/j.bej.2017.07.007>

¹³ K. S. Salem, N. K. Kasera, Md. A. Rahman, H. Jameel, Y. Habibi *et al.*, *Chem. Soc. Rev.*, **52**, 6417 (2023), <https://doi.org/10.1039/D2CS00569G>

¹⁴ A. Isaogai and M. Usuda, *Sen'i Gakkaishi*, **46**, 324 (1990)

¹⁵ Y. Liu, J. Chen, X. Wu, K. Wang, X. Su *et al.*, *RSC Adv.*, **5**, 34353 (2015),

<https://doi.org/10.1039/C5RA03300D>

¹⁶ C. W. Park, S. Y. Han, H. W. Namgung, P. N. Seo, S. Y. Lee *et al.*, *BioResources*, **12**, 5031 (2017),

<https://doi.org/10.15376/biores.12.3.5031-5044>

¹⁷ M. Brebu and C. Vasile, *Cellulose Chem. Technol.*, **44**, 353 (2010),

[https://www.cellulosechemtechnol.ro/pdf/CCT9\(2010\)/P.353-363.pdf](https://www.cellulosechemtechnol.ro/pdf/CCT9(2010)/P.353-363.pdf)

¹⁸ N. R. Rao, T. V. Rao, S. V. S. R. Reddy and B. S. Rao, *J. Radiat. Res. Appl. Sci.*, **8**, 621 (2015),

<https://doi.org/10.1016/j.jrras.2015.07.003>

¹⁹ Z. Xu, Q. Wang, Y. Feng, H. Han, Y. He *et al.*, *Ind. Crop. Prod.*, **222**, 119910 (2024),

<https://doi.org/10.1016/j.indcrop.2024.119910>